



Etched quantum dots for all-optical and electro-optical switches

Nathan Bickel*, Patrick LiKamWa

CREOL & FPCE, The College of Optics and Photonics, University of Central Florida, P.O. Box 162700, Orlando, FL 32816-2700, USA

Abstract

We present progress to date in the production of quantum dots etched from multiple quantum well structures for use in all-optical and electro-optical switches. Details of fabrication and comparisons to self-assembled quantum dot materials are described, and the direction of our continuing research is outlined.

© 2007 Elsevier Ltd. All rights reserved.

Keywords: Quantum dots; Quantum boxes; All-optical; Deep etching; Nanofabrication

1. Introduction

Quantum dots (QD) exhibit several distinct advantages over quantum wells. These include reduced spectral linewidth, controllable alpha parameter [1], and enhanced carrier transport [2], which are properties pertinent to the fabrication of devices for all-optical and electro-optical switching. However, the most successful approach for creating QD semiconductors is the Stranski–Krastanow self-assembled growth method. QD formed in this manner often exhibit significant size distribution and, therefore, a broadening of the absorption transitions. This fact renders self-assembled quantum dots (SAQD) less than suitable for use in electro-optical and all-optical switching devices, despite the high success of these structures in the fabrication of other optoelectronic devices such as quantum dot laser diodes [3] and quantum dot infrared photodetectors [4].

We propose to utilize an alternative scheme, by which layers of QD arrays are produced by electron beam lithography coupled with the reactive ion etching (RIE) of epitaxially grown multiple quantum wells (MQW). These etched quantum dot arrays show a high degree of size uniformity and, consequently, a low spread of the electron transitional energies. Several past attempts to capitalize on this technique [5,6] have not been pursued in

more recent times, because the high density of non-radiative defects that are created during the etching process result in low internal quantum efficiency for light emission and photon detection. Conversely, the non-radiative recombination is not a hindrance for electro-optic and all-optical devices, and could in fact be advantageous for fast device recovery times [7,8].

At further issue is the number of SAQD layers that can be stacked. This can be limited by strain accumulation in the active region which leads to a buildup of point defects in the QD layers and a degradation of internal quantum efficiency [9]. As a consequence, limitations on the number of SAQD layers would restrict the size of the active region and reduce the extent of the third order nonlinear effect imparted by the QD. One of the principle benefits of the etched quantum dots will be the ability to tailor the vertical dimension and composition of the structures through standard epitaxial deposition (MOCVD and MBE) of the MQW material. The formation of high quality, quantum well stacks with any particular number of layers can be readily achieved. This has the potential of allowing a structure which can realize a significant shift in the bandgap energy while utilizing a vertically applied field.

2. Material fabrication

Fabrication of the etched quantum dot structures begins with the deposition of 400 nm of silicon dioxide on the surface of the MQW wafer sample. A dual-system

*Corresponding author. Tel.: +1 407 595 3695; fax: +1 407 823 6880.
E-mail address: nbickel@creol.ucf.edu (N. Bickel).

PlasmaTherm 790 PECVD/RIE reactor is utilized, producing a film with good uniformity and roughness characteristics. This is followed by the spinning of a 70 nm coating of PMMA 950K electron beam resist. The desired dot array is then written using a Leica EBPG5000+ Electron Beam Lithographic System with the beam current at 500 pA, the dose set at $740 \mu\text{C}/\text{cm}^2$, and a 50 keV accelerating voltage. A solution of MIBK:IPA (1:3) was used as the developer to provide high contrast features. The sample was suspended motionless in the developer for 60 s, then rinsed in isopropyl alcohol for 30 s and rinsed again in DI water for an additional 45 s, and finally dried with N_2 gas.

After developing the electron beam resist, a 30 nm thick layer of chromium is evaporated onto the patterned area and lifted off, leaving behind an array of metal disks. These disks act as the etch mask for the SiO_2 layer, the uncovered portion of which is then etched using a CF_4 -based RIE process. This yields 400 nm high silicon dioxide pillars that are approximately 40 nm in diameter (Fig. 1). The pattern is then transferred into the GaAs/AlGaAs MQW employing a BCl_3 -based etching process, and carried out in an UNIAXIS ICP-RIE III–V reactor. The ICP-RIE system offers separate control of the plasma density and ion energy, allowing for highly anisotropic etching profiles. Following the III–V etching step, any metal or silicon dioxide that remains from the masking layer is removed and a planarization compound is applied for structural support of the semiconductor columns.

A scanning electron microscope (SEM) was used to image the nanopillar arrays and provide information on the etching profile, the pillar diameter and the pillar height. To date, we have produced arrays of GaAs nanopillars that have a diameter of approximately 43 nm and a height of 550 nm, as shown in Fig. 2. The arrays are laid out in a square lattice, with the smallest period achieved being 200 nm.

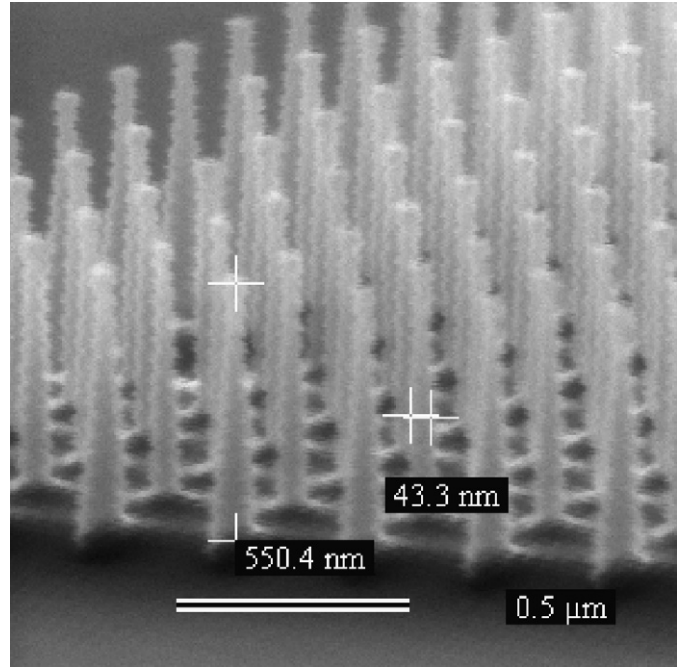


Fig. 2. SEM image of 43 nm gallium arsenide pillars etched in ICP-RIE reactor.

3. Discussion

In principle, the columns of semiconductor material which remain after the ICP-RIE etching process will contain a number of laterally confined quantum wells or quantum boxes (i.e., etched quantum dots). One of the indications that quantum confinement is present in the etched structures is a measurable shift of the photoluminescence spectrum compared with that measured from the as-grown material. This manifests as a move to higher photon energies and, for a particular material system and quantum well thickness, is dependent upon the lateral size of the etched quantum dot. For a GaAs/AlGaAs system at room temperature, the lateral dimensions need to be reduced to within a range of 20–30 nm to attain significant shift.

Patterned resist features and metal dot formation in this range of diameters can be accomplished with currently available electron beam lithography techniques and technology [10]. Since the MQW materials utilized in this project contain quantum wells that are buried deeply, the particular challenge to our work has been to realize a high aspect ratio coupled with a dot diameter that does not exceed 30 nm. Etch depths described to date have generally been very shallow, with columns ranging from 50 to 200 nm in height, placing the etched quantum dots very near the surface of the epitaxial layer [5,6]. Deeper etchings and aspect ratio's exceeding 10:1 have been reported, though the pillars were 100 nm in diameter or greater [11]. Our most recent results show GaAs pillars which exceed a 12:1 aspect ratio with pillar diameters approaching 40 nm (Fig. 2).

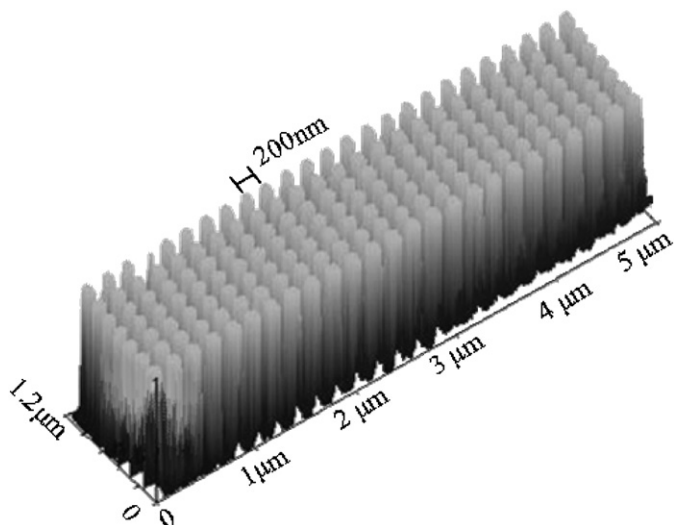


Fig. 1. AFM Image of silicon dioxide nanopillars on GaAs surface.

Highly anisotropic etching and high selectivity of the etch material over the masking material for both the SiO₂ and the GaAs/AlGaAs is crucial to the formation of small diameter, high aspect ratio semiconductor pillars. In the case of the oxide etching, the PlasmaTherm 790 tool is a parallel plate RIE system, without independent control of the plasma density and ion energy. This can be compensated for by balancing the residual pressure against the applied RF power. Extremely low residual pressure of 6 mTorr is matched to a moderate RF power of 125 W, with a tradeoff in a low, 16 nm/min etch rate. However, the result is good selectivity (~1:13) between the Cr mask and the SiO₂, and an almost 90° etch profile. The UNIAXIS ICP-RIE III-V reactor, used in etching GaAs and AlGaAs materials, has the advantage of an additional control parameter, which is the ability to separately manipulate the plasma density and ion energy. Despite this added control, tradeoff between the etch rate and profile is still necessary. Achieving a 90° etch profile is of predominate importance and therefore etch rate is sacrificed. Since the ICP independently provides a high-density plasma source, though, the etch rate is still in the range of 150–250 nm/min. Selectivity between the etch mask and the GaAs is not as critical as in the case of the SiO₂ pillar formation due to the extreme thickness of the SiO₂ masking layer.

The dot density for the etched quantum dots discussed above is comparable to that which is achievable for SAQD (10^9 – 10^{11} cm⁻²) in GaAs-based systems [12]. For etched quantum dots with a 30 nm diameter and a 100 nm center-to-center spacing in a square lattice, the dot density is approximately 10^{10} cm⁻². Currently, we have produced dots with an in-layer density of 0.25×10^{10} cm⁻². As noted in Section 1, however, the active region extends into the third dimension through layer stacking, and whereas the number of SAQD layers in a stack is often limited due to the effects of strain accumulation [9], the number of etched quantum dot layers in a stack is only restricted by the number of quantum well layers that can be grown. By employing standard epitaxial deposition (MOCVD and MBE), almost any number of quantum wells is practical. For instance, MQW stacks consisting of 400-wells have been grown [13]. Notably, it is difficult to set a precise limit on the number of good quality SAQD layers that can be formed in a stack, as this is dependent on many parameters, including barrier layer thickness and the material system employed. Overall these parameters will be primarily influenced by the intended application of the epitaxial material. Finally, further improvement of the in-plane packing density is already being implemented and can be accommodated by reducing the center-to-center spacing, as well as by shifting from a square lattice to a hexagonal lattice.

4. Future work

To date, we have produced arrays of GaAs nanopillars that have a diameter of approximately 43 nm and a height

of 550 nm. Currently, we are moving toward the further improvements in the pillar diameter and aspect ratio which are necessary to realize etched quantum dots with significant quantum confinement in the lateral direction. Once proven, these fabrication techniques will be transferred to forming quantum dots from etched GaAs/AlGaAs quantum well materials. Characterization of the optical properties and introduction of the etched quantum dots into electro-optical devices will follow.

Acknowledgment

We would like to acknowledge the support from the US Army Research Office, Grant no. W911NF-05-1-0223.

References

- [1] R. Sahara, M. Matsuda, H. Shoji, K. Morito, H. Soda, Proposal for quantum-dot electroabsorption modulator, *IEEE Photon Technol. Lett.* 8 (1996) 1477–1479.
- [2] G.H. Kim, D.A. Ritchie, M. Pepper, G.D. Lian, J. Yuan, L.M. Brown, Transport properties of two-dimensional electron gases containing InAs self-assembled dots, *Appl. Phys. Lett.* 73 (1998) 2468–2470.
- [3] P. Bhattacharya, S. Ghosh, S. Pradhan, J. Singh, Z.-K. Wu, et al., Carrier dynamics and high-speed modulation properties of tunnel injection InGaAs–GaAs quantum-dot lasers, *IEEE J. Quantum Electron* 39 (2003) 952–962.
- [4] Y.-C. Cheng, S.-T. Yang, J.-N. Yang, W.-H. Lan, L.-B. Chang, L.-Z. Hsieh, Fabrication of a far-infrared photodetector based on InAs/GaAs quantum dot superlattices, *Opt. Eng.* 42 (2003) 119–123.
- [5] L. Davis, K.K. Ko, W.-Q. Li, H.C. Sun, Y. Lam, T. Brock, et al., Photoluminescence and electro-optic properties of small (25–35 nm diameter) quantum boxes, *Appl. Phys. Lett.* 62 (1993) 2766–2768.
- [6] T.D. Bestwick, M.D. Dawson, A.H. Kean, G. Duggan, Uniform and efficient GaAs/AlGaAs quantum dots, *Appl. Phys. Lett.* 66 (1995) 1382–1384.
- [7] E. Lugagne Delpon, J.L. Oudar, N. Bouche, R. Raj, A. Shen, N. Stelmakh, et al., Ultrafast excitonic saturable absorption in ion-implanted InGaAs/InAlAs multiple quantum wells, *Appl. Phys. Lett.* 72 (1998) 759–761.
- [8] H.S. Loka, P.W.E. Smith, Ultrafast all-optical switching in an asymmetric Fabry–Perot device using low-temperature grown GaAs, *IEEE Photon Technol. Lett.* 10 (1998) 1733–1735.
- [9] N.N. Ledentsov, M. Grundmann, F. Heinrichsdorff, D. Bimberg, V.M. Ustinov, A.E. Zhukov, et al., Quantum-dot heterostructure lasers, *IEEE J. Select. Top. Quantum Electron* 6 (2000) 439–451.
- [10] C. Vieu, F. Carcenac, A. Pepin, Y. Chen, M. Mejias, A. Lebib, et al., Electron beam lithography: resolution limits and applications, *Appl. Surf. Sci.* 164 (2000) 111–117.
- [11] S. Varoutsis, S. Laurent, I. Sagnes, A. Lemaître, L. Ferlazzo, C. Meriadec, et al., Reactive-ion etching of high-Q and submicron-diameter GaAs/AlAs micropillar cavities, *J. Vac. Sci. Technol. B* 23 (2005) 2499–2503.
- [12] D. Leonard, M. Krishnamurthy, C.M. Reaves, S.P. Denbaars, P.M. Petroff, Direct formation of quantum-sized dots from uniform coherent islands of InGaAs on GaAs surfaces, *Appl. Phys. Lett.* 63 (1993) 3203–3205.
- [13] S.D. Ganichev, E.L. Ivchenko, S.N. Danilov, J. Eroms, W. Wegscheider, D. Weiss, et al., Conversion of spin into directed electric current in quantum wells, *Phys. Rev. Lett.* 86 (2001) 4358–4361.